Theoretical and experimental correlations of gas dissolution, diffusion, and thermodynamic properties in determination of gas permeability and selectivity in supported ionic liquid membranes

Gan, Q., Zou, Y., Rooney, D., Nancarrow, P., Thompson, J., Liang, L., & Lewis, M. (2011). Theoretical and experimental correlations of gas dissolution, diffusion, and thermodynamic properties in determination of gas permeability and selectivity in supported ionic liquid membranes. Advances in Colloid and Interface Science, 164(1-2), 45-55. DOI: 10.1016/j.cis.2011.01.005

Published in:
Advances in Colloid and Interface Science

Advances in Colloid and Interface Science 164 (2011) 45–55

Contents lists available at ScienceDirect

Advances in Colloid and Interface Science

journal homepage: www.elsevier.com/locate/cis

Theoretical and experimental correlations of gas dissolution, diffusion, and thermodynamic properties in determination of gas permeability and selectivity in supported ionic liquid membranes

Quan Gan *, Yiran Zou, David Rooney, Paul Nancarrow, Jillian Thompson, Lizhe Liang, Moira Lewis

School of Chemistry & Chemical Engineering, Queen's University Belfast, Belfast BT9 5AG, UK

ARTICLE INFO

Available online 1 February 2011

Keywords:
Gas separation
Ionic liquids
Gas membrane separation
Supported ionic liquid membrane
Solution diffusion mechanism

ABSTRACT

Supported ionic liquid membranes (SILMs) has the potential to be a new technological platform for gas/organic vapour separation because of the unique non-volatile nature and discriminating gas dissolution properties of room temperature ionic liquids (ILs). This work starts with an examination of gas dissolution and transport properties in bulk imidazulium cation based ionic liquids [$C_n$mim][NTf2] (n = 2.4, 6, 8.10) from simple gas H_2, N_2, to polar CO_2, and C_2H_6, leading to a further analysis of how gas dissolution and diffusion are influenced by molecular specific gas-SILMs interactions, reflected by differences in gas dissolution enthalpy and entropy. These effects were elucidated again during gas permeation studies by examining how changes in these properties and molecular specific interactions work together to cause deviations from conventional solution–diffusion theory and their impact on some remarkably contrasting gas perm-selectivity performance. The experimental perm-selectivity for all tested gases showed varied and contrasting deviation from the solution–diffusion, depending on specific gas-IL combinations. It transpires permeation for simpler non-polar gases (H_2, N_2) is diffusion controlled, but strong molecular specific gas-ILs interactions led to a different permeation and selectivity performance for C_2H_6 and CO_2. With exothermic dissolution enthalpy and large order disruptive entropy, C_2H_6 displayed the fastest permeation rate at increased gas phase pressure in spite of its smallest diffusivity among the tested gases. The C_2H_6 gas molecules "peg" on the side alkyl chain on the imidazulium cation at low concentration, and are well dispersed in the ionic liquids phase at high concentration. On the other hand strong CO_2-ILs affinity resulted in a more prolonged "residence time" for the gas molecule, typified by reversed CO_2/N_2 selectivity and slowest CO_2 transport despite CO_2 possess the highest solubility and comparable diffusivity in the ionic liquids. The unique transport and dissolution behaviour of CO_2 are further exploited by examining the residing state of CO_2 molecules in the ionic liquid phase, which leads to a hypothesis of a condensing and holding capacity of ILs towards CO_2, which provide an explanation to slower CO_2 transport through the SILMs. The pressure related exponential increase in permeations rate is also analysed which suggests a typical concentration dependent diffusion rate at high gas concentration under increased gas feed pressure. Finally the strong influence of discriminating and molecular specific gas-ILs interactions on gas perm-selectivity performance points to future specific design of ionic liquids for targeted gas separations.

Contents

* Corresponding author. Tel.: +44 28 90974463.
E-mail address: q.gan@qub.ac.uk (Q. Gan).

0001-8686/$ – see front matter © 2011 Elsevier B.V. All rights reserved.
doi:10.1016/j.cis.2011.01.005

1. Background

Research in room temperature ionic liquids (RTILs) started with main focus on exploring the unique and specific solvent and catalytic properties in homogeneous or heterogeneous catalysis [1,2], aiming for greater selectivity, specificity and yield at reduced environmental liabilities. Many ionic liquids also exhibit unique solubility, transport and separation properties [3,4], which led to spreading research in using ionic liquids as a selective separation media for gas separation, enrichment and solvent extraction. There exists a great interest in exploitation of RTILs for CO_2 capture and storage due to its distinctively large solubility in a variety of ionic liquids in comparison to other simple gases. A strong interest has also been developing in olefin–paraffin separation using RTILs where transport is facilitated by partially polarised silver ions [5,6]. On technological and process development, the negligible volatility of ionic liquids makes them a good choice for supported liquid membrane. The main difficulty of conventional supported liquid membrane lies with preparing a stable and immobilized liquids film on a support solid media because the liquids slowly evaporate, destabilising selective properties and flux through the membrane, also causing contamination to feed gas streams [5,7,8]. Non-volatile and selective ionic liquids supported on porous membranes have distinctive advantages because the ionic liquids do not evaporate, and their high viscosity may provide additional stability to pressure displacement from the solid porous support. Most reported studies of SILM used microporous membrane as support, and gas transport/separation studies were conducted in single gas feed system operating under low pressure differential to avoid displacement of ionic liquids [9,10]. These studies succeeded in obtaining information and knowledge in relation to gas solubility, diffusivity and permeability under low gas phase pressure. However, gas solubility and diffusion behaviour in solvent at increased concentration under high gas phase pressure may deviate from the standard dissolution and diffusion behaviour, especially when gas-solvent molecular interactions may further influence the transport process. Previously we reported a study of ionic liquids supported on nano-pore membrane which exhibited extraordinary membrane stability under high gas phase pressure [11]. This work aims to built on the process development by providing a theoretical analysis of gas dissolution and transport in the pressure stable SILMs.

Many recent works on gas permeability and selectivity involve CO_2 because of its strong solubility in most ionic liquids. Park et al. reported gas permeability of CO_2, H_2S, and CH_4 in a poly(vinylidene fluorolide) supported [C_4mim][BF_4] membrane. Ideal selectivity for the CO_2/CH_4 gas pair was calculated by single gas permeation at 40 [12]. Bara et al. used poly(ethersulfone) (PES) supported [NTf_2] ILs containing perfluoroalkyl substituents, and reported the highest selectivity of 19 and 27 for CO_2/CH_4 and CO_2/N_2 respectively [13,14]. Sulphur dioxide, which has similar molecular structure of CO_2, was also studied in a PES SILM using various ILs. Ideal selectivity of SO_2/CH_4 was found to be 144 in [C_4mim][BF_4] at 25 °C [15]. Pennline et al. presented CO_2 removal from fuel gas in membrane gas separation using polyethylsulfone to support two ILs, [C_6mim][NTf_2] and [C_4mim][NO_3]. Ideal selectivity of CO_2/H_2 was found to be 6 and 5.20 respectively at 310 K [16]. Similar work was carried out by Myers et al., who found the selectivity of CO_2/H_2 in [C_3NH_2mim][NTf_2] SILM increased with increasing temperature from 37 to 85 °C, due to the larger activation energy of complex [17]. Ionic liquids had also been studied in the separation of CO_2 from flue gases emitted from fossil-fuel combustion operations [18], due to its high solubility in ionic liquids. In the CO_2/H_2 system, a CO_2 selectivity of 30–300 was observed in [C_4mim][PF_6] [19].

Scovazzo et al. [5] studied RTIL-membranes made from the water stable anions: bis(trifluoromethanesulfonyl)amide $[NTf_2]^-$, trifluoromethanesulfone $[CF_3SO_3]^-$, chloride $[Cl]^-$, and dicyanamide $[dca]^-$. The CO_2 permeability on the SILMs are related to the CO_2 solubilities in ILs. The flux and ideal selectivities for the gas pairs CO_2/N_2 from 15 (for $[[Cl]^-]$) to 61 (for $[dca]^-$); and CO_2/CH_4 ideal selectivities range from 4 (for $[[Cl]^-]$) to 20 (for $[dca]^-$). Recently, Scovazzo et al. reported long-term continuous mixed gas separation selectivity on SILMs [20]. It was found mixed gas operation did not reduce the advantageous gas separation selectivities, compared with single gas ideal selectivity; membrane continued to give advantageous operations even under dry gas feed conditions; and long-term stability of more than 106 days confirmed in continuous flow operations without any detectable performance loss.

Solution–diffusion theory has been the backbone theory for gas transport through dense nonporous membranes, which has also been intensively evoked for SILM studies. However, uncertainty and discrepancy persist in relating the independently measured gas solubility/diffusivity/thermodynamic data in bulk ILs to observed gas permeation and separation performance in SILMs, which are often complicated by the complex molecular interactions between diffusing gas molecules and molecules of ionic liquids, which are more complex in structure and property performance than simple solvents. This weak link has been largely neglected so far but needs to be addressed more systematically and in depth so as to catch up with the fast research progress in SILM technology and process development. Therefore it is the main aim of this work to provide such a framework analysis of the interrelations between gas dissolution/diffusion properties and gas perm-selectivity in SILMs. It is necessary to state that the scope and accuracy of such an analytical attempt may be constrained and dependent on the availability and experimental accuracy of data on gas solubility and diffusivity. The limited understanding of gas-ionic liquid interactions at molecular level can be another limiting factor, which often leads to non-ideal behaviour of gas dissolution and concentration dependent diffusion.

2. Materials and experimental methods

2.1. Materials

Thin-film cellulose acetate nanofiltration membrane discs were purchased from Sterlitech Corporation (YMHLSP1905). The key relevant membrane parameters are given in Table 1. Scanning electron microscope (JEDL-6400, Link Analytical) showed the membrane has an asymmetric structure and a total thickness of 167 ± 2 μm. The membrane is originally designed for acid purification, alcohol purification, BOD/COD reduction, ethylene glycol purification, heavy metal removal, desalting and sugar fractionation. As a nanofiltration

Table 1
Key membrane parameters and chemical/physical properties of ionic liquids used in this work.

Membrane				
Designation	Thickness (μm)	Ionic rejection	pH Range at 25 °C	Typical water Flux (m^3/m^2 bar)
DK nanofiltration	167 ± 2	98% $MgSO_4$	2 – 14	22/100

Ionic liquids properties at T=298K			
Ionic liquids	Viscosity (cP)	Density (g cm^{-3})	Molar volume (cm^3mol^{-1})
$[C_2mim][NTf_2]$	54.1	1.52	258.0
$[C_4mim][NTf_2]$	69.0	1.44	292.0
$[C_{10}mim][NTf_2]$	124.0	1.27	404.1
$[C_4mim][OTF]$	93.2	1.29	230.9
$[C_4mim][BF4]$	103.0	1.21	189.3
$[C_4mim][PF6]$	320.3	1.35	207.8

Illustration of cation molecular structure $[C_4mim]^+$, $[C_{10}mim]^+$, and anion $[OTF]^-$, $[NTf2]^-$, $[BF4]^-$

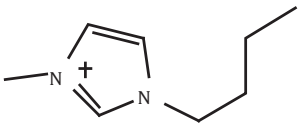

1-methyl-3-butylimidazolium

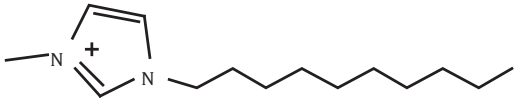

1-methyl-3-decylimidazolium

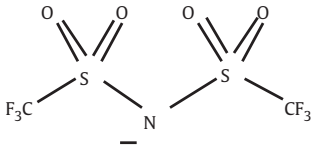

Bistrifluoromethanesulfonimide

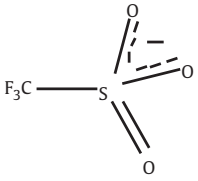

Trifluoromethanesulphonate

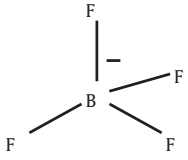

Tetrafluoroborate

membrane it contains functionalised groups carrying charges on the polymer chains. The membrane is compatible with chemical organic groups aliphatic hydrocarbons, halogenated hydrocarbons, alcohol, and acids, but unstable when in contact with aromatic hydrocarbons, asymmetric halogenated hydrocarbons, ketones, ethers, and esters.

All the ionic liquids used in this study were synthesised in QUILL (Queen's University Ionic Liquid Laboratory) [21]. NMR were used to analyse bromide residual and other impurities as minute amount impurities may have significant influence on thermodynamic and thermo-physical properties of the ionic liquids. The most relevant physical and chemical properties of the ionic liquids used in this work are also presented in Table 1.

2.2. Gas solubility measurement

An isochoric saturation technique was used for gas solubility measurement. Detailed procedures were reported in Ballerat-Busseroles et al. [22,55]. Briefly. a known quantity of gaseous solute is put in contact with a precisely determined quantity of degassed solvent at a constant temperature inside an accurately known volume. When thermodynamic equilibrium is attained, the pressure above the liquid solution is constant and is directly related to the solubility of the gas in the liquid (Fig. 1).

2.3. Preparation of supported ionic liquid membranes and their stability

Detailed preparation of the supported ionic liquid membranes was reported previously [11]. Briefly the pristine nanofiltration membranes were soaked in the ionic liquids for 24 h. The excess ILs on the surface of the membrane was carefully removed by clean cotton tissue. The nanofitration membranes have excellent affinity and wetability in the ionic liquids with 45% of IL weight uptake after soaking. The SILMs are stable under pressure and over long operating time with practically little loss of the ionic liquids.

The stabilising mechanism based on the interactions between cations/anions with the charged NF membrane materials in a nano spatial scale is not entirely clear. It is speculated that strong cationic/

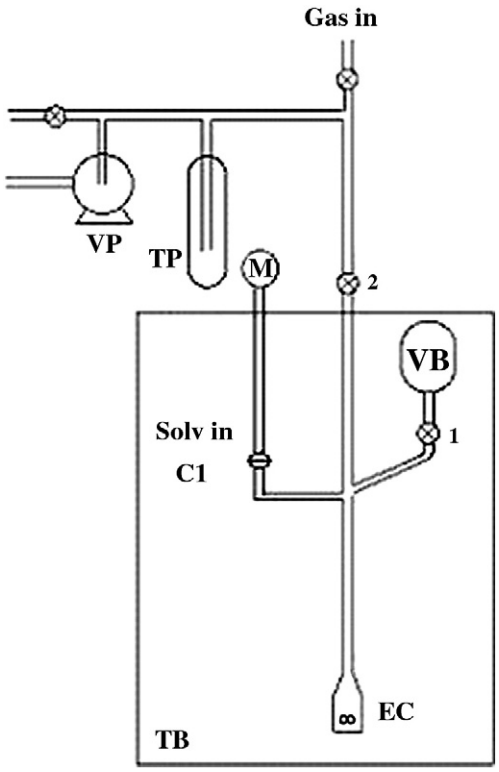

Fig. 1. Gas solubility measurement apparatus (TB: thermo bath; EC: equilibrium cell; VB: calibrated gas bulb; M: manometer; TP: cold trap).

anionic interactions with functional groups present at the nanopore walls within a radial dimension of 1–10 Å may form structured arrangement of the cations/anions within the nanopore networks. Such a formation could give rise to unique gas transport and separation properties different to ionic liquids in bulk liquid conditions.

2.4. Gas permeation studies

The experimental apparatus for the gas transport measurement is composed of a gas cylinder, pressure gauge, pressure sensor, gas reservoir, membrane separation cell, cold trap and the vacuum pump, as show in the process diagram in Fig. 2. All cells, tubes and valves are designed for high-pressure application. The flat sheet NF membrane was mounted in a SEPA stainless steel membrane filtration cell (Sterlitech Corporation) with a holding volume of 300 mL and an effective membrane permeation area of 16.9 cm^2. The SEPA cell is placed in a temperature controlled water bath to maintain a constant temperature during gas permeation. All gas permeation tests were conducted at constant T = 303 K.

3. Results and discussion

3.1. Gas solubility in ionic liquids

Since Blanchard et al. firstly reported gas solubilities in ionic liquids in 2000 [23], gas solubilities in many common ionic liquids are reported [24–27]. The literature data obtained from the IUPAC (International Union of Pure and Applied Chemistry) database contains solubility data for fifteen gases in 27 ionic liquids. It is also possible to develop correlations which can be used to predict gas solubility in ionic liquids [28]. Among all gases, carbon dioxide is the most intensively reported due to its outstanding solubility in most ionic liquids. It was generally found that gas molecules with dipole movement such as carbon dioxide, sulphur dioxide, and nitrous oxide have the highest solubilities and strongest interactions with the ionic liquids, followed by ethylene and ethane. Gases such as oxygen, nitrogen, hydrogen, and carbon monoxide have very low solubilities and low interactions with ionic liquids [29,30]. Based on recent experimental, spectroscopic and molecular simulation studies, it transpires that anions dominate the interactions with the gas molecular, with the cations playing a secondary role [31–34]. Gas solubility data pertinent to many gas separations are still incomplete. For engineering applications, accurately measured gas solubility at a pressure greater than atmosphere pressure is important but difficult to obtain for some experimental methods such as volumetric method and gravimetric method.

Solubility of CO, CO_2, CH_4 C_2H_6 were measured in this work using the isochoric saturation method. Henry's law constant for gas dissolution can be calculated in theory from the mole fraction solubilities as:

$$K_H \equiv \lim_{x_2 \to 0}\left(\frac{f_2\left(p_{eq}, T_{eq}, y_2\right)}{x_2}\right) = \lim_{x_2 \to 0}\left(\frac{\phi_2\left(p_{eq}, T_{eq}\right)p_{eq}}{x_2}\right) \cong \left(\frac{\phi_2\left(p_{eq}, T_{eq}\right)p_{eq}}{x_2}\right)$$

Detailed experimental procedure and calculation procedure in relation to the above equation can be found in Anthony et al. [34]. H_2 and N_2 have very low solubility in the ionic liquids, and difficult to measure accurately by the method used in this work. Our literature survey found only one reported H_2 solubility data [35] in [C_4mim][NTf_2], and no literature data available at all on N_2 solubility in [C_4mim][NTf_2], except in ionic liquids [C_4mim][BF_4] [55]. In the absence of experimental data, the thermodynamic model, COSMO-RS, was used for *a priori* prediction of gas solubility in ionic liquids. Briefly, COSMO calculations were performed on each individual ion or molecule using the TURBOMOLE [36] quantum chemistry package. Computations were carried out on the density functional theory (DFT) level, using the BP functional [28,37] with a triple-valence polarised basis set (TZVP) [38] Where applicable, optimised radii [39] were used in the COSMO calculation (H = 1.30, C = 2.00, N = 1.83, O = 1.72, F = 1.72, S = 2.16, Cl = 2.05, Br = 2.16, I = 2.32); otherwise, 1.17 × vdW radii were used. To generate gas solubility calculations, the COSMO files were imported into COSMOthermX software and a ternary system (gas + cation + anion) was used as the basis for the calculations, as recommended by COSMOlogic [40]. The calculated mol fraction of gas in the liquid phase was then converted to mol fraction for a binary system (gas + ionic liquid).

Experimental and predicted Henry constant and gas mole fraction for H_2, N_2, CO, CO_2, CH_4 C_2H_6 in ionic liquid [C_4mim][NTf_2] are presented in Table 2. The CO_2 solubility is one magnitude higher than other gases, and C_2H_6 solubility is also one order of magnitude higher than non polar H_2 and N_2.

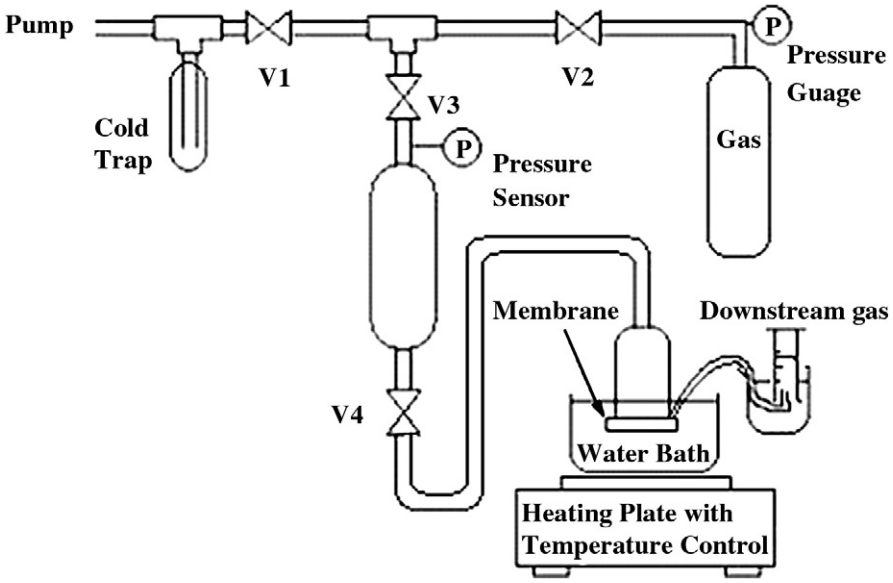

Fig. 2. Flow diagram for gas permeation test through the SILMs.

Table 2
H_2, N_2, CO, CO_2, CH_4 and C_2H_6 gas solubilities in [C_4mim][NTf_2] expressed as Henry's law coefficient K_H and mole fraction x.

T/K	$K_H/10^5$Pa	$x/10^{-3}$	AAD	T/K	$K_H/10^5$Pa	$x/10^{-3}$	AAD
[C_4mim][NTf_2] + CO_2 (experimental				[C_4mim][NTf_2] + C_2H_6 (experimental)			
303.2	35.46	28.20	0.0%	303.7	105.7	9.465	0.1%
313.1	42.08	23.77	0.1%	313.8	118.3	8.455	0.6%
323.0	49.42	20.23	0.1%	324.2	140.2	7.133	0.1%
332.9	57.35	17.44	0.0%	334.0	165.5	6.042	1.3%
[C_4mim][NTf_2] + CH_4 (experimental)				[C_4mim][NTf_2] + CO (experimental)			
303.2	345.5	2.894	0.8%	303.2	653.8	1.529	4.0%
313.1	369.7	2.705	1.6%	313.1	659.5	1.516	3.0%
323.1	414.2	2.415	2.1%	323.0	732.3	1.366	1.4%
333.1	419.3	2.385	4.3%	333.0	816.8	1.224	0.1%
[C_4mim][NTf_2] + N_2 (COSMO prediction)				[C_4mim][NTf_2] + H_2 (COSMO prediction)			
303.0	537.5	0.19		303.0	2016.1	0.50	
313.0	607.5	0.17		313.0	2140.2	0.47	
323.0	680.1	0.15		323.0	2261.3	0.45	
333.0	754.5	0.13		333.0	2379.2	0.43	

In Table 2, Average Absolute Deviation (AAD) was calculated based on the equation:

$$AAD = 100\left(\sum_{i=0}^{n}\frac{\left|x_i - x_i^{ref.}\right|}{x_i^{ref.}}\right) = 100\left(\sum_{i=0}^{n}|\delta_i|\right)$$

An average of ten sample data was measured at each temperature.

CO_2 solubility in other ionic liquids were also measured for [C_4mim][BF_4] and [C_4mim][PF_6] which possess the same cation but differ in anions, and also in ionic liquids [C_2mim][NTf_2], [C_6mim][NTf_2] and [C_8mim][NTf_2] which all share the same $[NTf2]^-$ anion but differ in the length of the side alkyl chain on the cation $[C_n mim]^+$. Henry's law constant and dissolved gas mole fraction are presented in Table 3 to illuminate the effect of cation and anion on the gas solubility. Anions had strong influence on gas solubility and the results shows that CO_2 solubility in [C_4mim] cation based ionic liquids followed the order [BF_4]<[PF_6]<[NTf_2], similar to data reported by Anthony et al. [29]. Cations difference had a lesser effect, and CO_2 solubility increases slightly with increasing length of the alkyl side chain on the imidazolium ring. It is thought that this may be due to entropic reasons, as there may be more free volume within the longer chain ILs, which corresponds to a proportional relationship with the molar volume of ionic liquids [41,42]. Fig. 3 shows that results obtained from this work corroborates well with data reported in literature employing same or different measurement methods [29,42,43].

3.2. Gas diffusivity in bulk ionic liquids and in SILM

Directly measured gas diffusivity in bulk ionic liquids are largely incomplete, partially due to experimental difficulties to ascertain slow gas diffusion rate in highly viscous liquids. A time-lag method [44,45] was developed for predicting gas diffusivity through SILMs. Both gas solubility and diffusivity are calculated from the equation below from the same set of flux-time data, which does not distinguish the effect of solubility and transport on the permeation rate.

$$\frac{Q_t}{Lc_i} = \frac{Dt}{L^2} - \frac{1}{6} - \frac{2}{\pi}\sum\frac{(-1)^n}{n^2}\exp\left[\frac{-Dn^2\pi^2 t}{L^2}\right]$$

where c_i is the concentration on the feed side and n is an integer. A curved plot can be observed initially in the transient state but this becomes linear with time as steady-state conditions are attained. When $t \Rightarrow \infty$, the exponential term can be neglected and it simplifies to:

$$Q_t = \frac{Dc_i}{L}\left(t - \frac{L^2}{6D}\right)$$

If the linear plot of $Q_t/(Lc_i)$ versus t is extrapolated to the time axis, the resulting intercept, θ, is called the time lag, and the diffusion coefficient can be calculated when the membranes thickness is known.

A number of theoretical prediction of gas diffusivity in liquids is available. The best known Einstein's equation can be applied to molecular diffusion without accounting for interactions between the

Table 3
CO_2 Henry's law constant and mole fraction in [$C_n$mim] cation (n = 2.4,6.8) based ionic liquids. T = 303 K P = 1.013 bar.

Ionic liquid	$K_H/10^5$Pa	$x/10^{-3}$
[C_4mim][NTf_2]	35.5	0.031
[C_4mim][BF_4]	60.8	0.016
[C_4mim][PF_6]	56.5	0.014
[C_2mim][NTf_2]	39.1	0.027
[C_6mim][NTf_2]	35.0	0.029
[C_8mim][NTf_2]	31.0	0.033

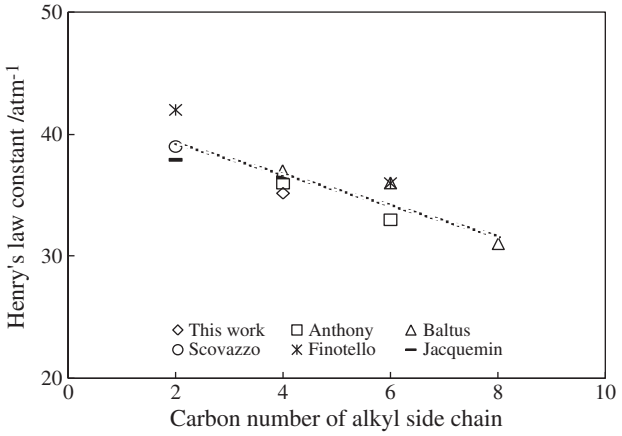

Fig. 3. Correlation of Henry's law constant for carbon dioxide in [$C_n$mim][NTf_2] (n = 2.4,6.8) ionic liquids.

diffusing molecules and/or with the molecules of the diffusion solvent media.

$$D_{12} = \frac{kT}{n\pi a_1 \mu_2} \qquad 4 \le n \le 6$$

According to Einstein's equation, the diffusion coefficient of solutes in a liquid is directly proportional to the reciprocal of the molecular radius of the diffusing solute.

The Wilke–Chang expression [46] is one of the widely used empirical correlations for estimating gas diffusion coefficients in liquids which take consideration of molecular interactions and properties of both diffusing molecule and that of the diffusion liquid media.

$$D = \left[7.48 \times 10^{-8}\right] \frac{T\sqrt{\alpha M_2}}{\mu_2 \overline{V}_1^{0.6}} \qquad \alpha = 0.15$$

whereas, $\overline{V}_1$ is the molar volume of the gas solute at its normal boiling point, α is the association constant which accounts for gas-liquid interactions, M_2 refers to the molecular weight of the solvent.

Scheibel correlation [47] modified the Wilke–Chang correlation to eliminate the association factor α:

$$D_{12} = |C| \frac{T\left(1 + \left(3\frac{\overline{V}_2}{\overline{V}_1}\right)^{2/3}\right)}{\mu_2 \overline{V}_1^{1/3}} \qquad C = 8.2 \times 10^{-8}$$

where $\overline{V}_2$ is the molar volume of the solvent. This equation is developed to eliminate solvent association factor in Wilke–Chang correlation by introducing molar volumes to account for solvent effects.

Although the empirical models have been widely used to predict gas solute diffusivity in water and simple solvents, their applicability and accuracy in predicting gas diffusion coefficient in ionic liquids has yet to be systematically examined. In this work, measured gas diffusivity data for O_2 and CO_2 in bulk ionic liquids from literature [33,45,48] are correlated to the calculated values of diffusivity based on Wilke–Chang and Scheibel model respectively, and the correlation are presented in Figs. 4 and 5. Morgan [45] and Buzzeo's [48] data correlate well with both equations. However, Shiflett's [33] data were around 50% lower than predicted values. The deviation is possibly due to the different methods used for measuring the diffusivity. Morgan and Buzzeo used the time-lag method on a supported ionic liquid membrane, while Shiflett used a one-dimensional diffusion model

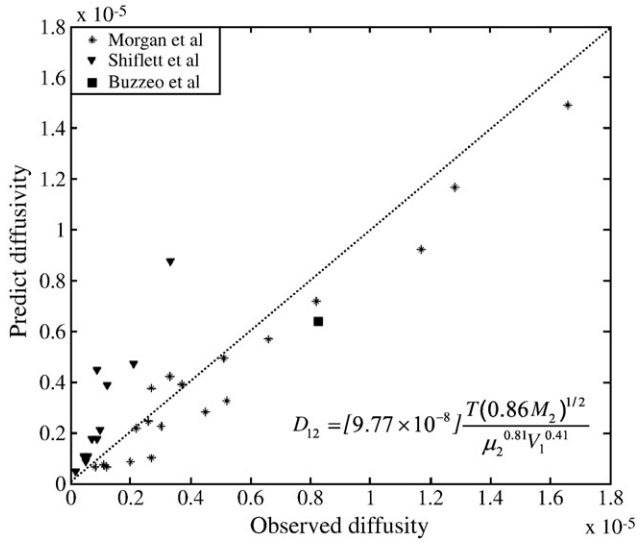

Fig. 4. Diffusion coefficient prediction and correlation using Wilke–Chang correlation.

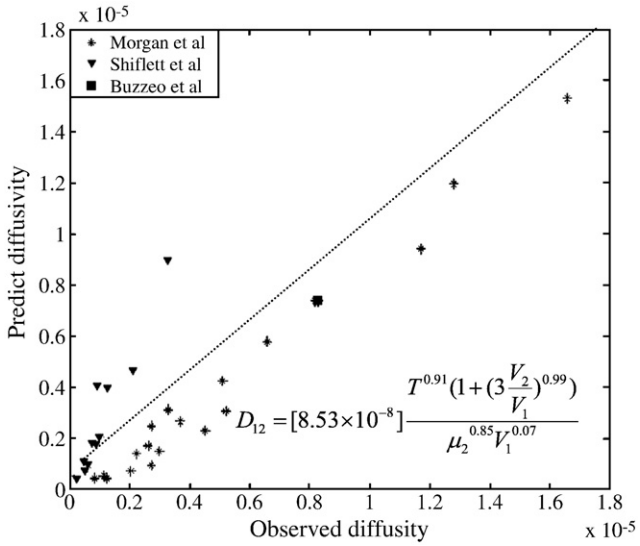

Fig. 5. Diffusion coefficient prediction and correlation using Scheibel correlation.

based on mass transfer [49]. The model in Sheflett's work used the following assumptions: (1) gas concentration in ionic liquid is a very low, so the thermophysical properties of the solution do not change; (2) temperature and pressure kept constant during dissolution; (3) thermodynamic equilibrium is instantly established on the boundary thin layer with a saturation concentration, which the concentration is constant all the time; (4) gas dissolves in one-dimensional diffusion process. These assumptions are reasonable for non polar gas species (H_2, N_2, O_2, and CO) which have low solubility and low interactive salvation enthalpy and entropy. Also Sheflett's data were measured across a much wide temperature and pressure range from 283.15 to 348.15 K and from 0.10 to 20.0 bar, whilst Morgan and Buzzeo's data can only be obtained at atmospheric pressure because of the pressure instability of their SILMs supported on micron-pore membranes.

Based on the knowledge of ionic liquid viscosity and molar volume presented in Table 1, the Wilke–Change and Scheibel correlations were used to calculate gas diffusion coefficients for H_2, N_2, CH_4, C_2H_6 and CO_2 in a number of ionic liquids. Liquid molar volume and molecular diameter of the gas species are also presented in the table for reference [50].

The calculated values of the diffusion coefficients followed the order: $H_2 > N_2 > CO_2 > CH_4 > C_2H_6$ within all three ionic liquids. This order of diffusivity value is in agreement with Einstein predications based on molecular weight/size. In comparison to diffusion coefficient values in solid polymers reported in literature [51–54], the values of these diffusion coefficients in bulk ionic liquids are one order of magnitude higher than in polyethylene, two order high than in PVC and polyimide, but one order of magnitude lower than some new novel polymers such as PDMS and PTMSP.

3.3. Permeation and selectivity of H_2, N_2, CO_2, CH_4 C_2H_6

Steady state permeability of hydrogen, carbon dioxide, nitrogen, methane and ethane through the [C_4mim][NTf_2] supported ionic liquid membrane are presented in Fig. 6. The steady state permeability were obtained after an initial “time lag” stage during which the SILM was saturated with gases before the onset of gas permeation which was observed to be steady with time. The high stability of the SILM supported on the nano-pore membrane enabled steady flux at high pressures relevant to industrial applications. Gas permeability increased exponentially for all five gases with increasing gas feed pressure, with ethane leading the faster increase followed by nitrogen,

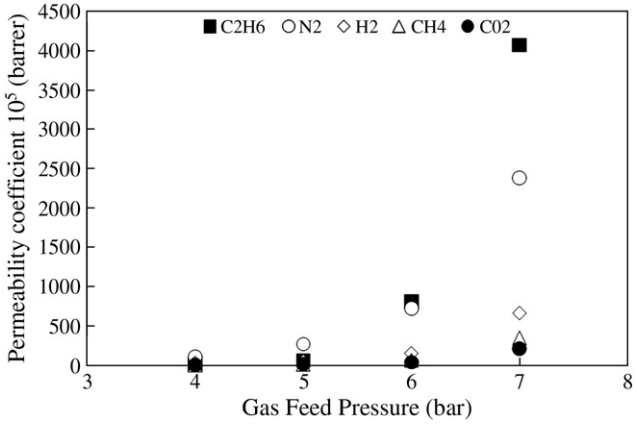

Fig. 6. Steady state gas flux through [C_4mim][NTf_2] SILM membrane.

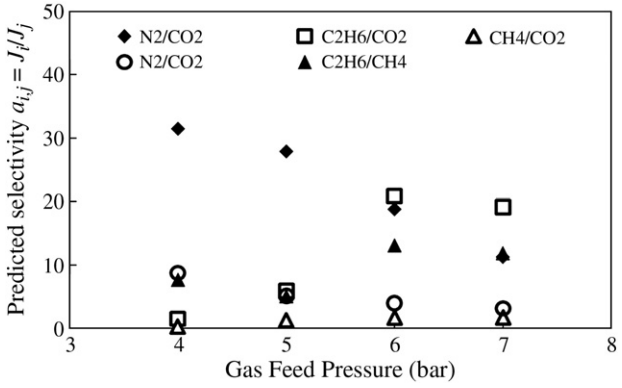

Fig. 7. Predicted selectivity based on single gas permeation measurement for gas pair N_2/CO_2, C_2H_6/CO_2, CH_4/CO_2, CH_4/N_2 based on experimental gas permeation data.

hydrogen, methane and carbon dioxide. The higher ethane permeability is rather remarkable given ethane has the lowest diffusivity and a solubility 3 time less than CO_2. It is also interesting to note N_2 and H_2 permeates faster than CO_2 in despite of very low solubility in the ionic liquid.

The calculated separation factor or selectivity based on single gas flux rate is calculated for gas pairs N_2/CO_2, C_2H_6/CO_2, CH_4/CO_2, CH_4/N_2. The gas pairs exhibit best separation ratio at lower pressure with the two exceptions all involving C_2H_6. The selectivities are compromised when gas fluxes increased, a typical scenario associated with gas separation by most polymeric membranes. CO_2 exhibits the best selectivity against other gas with a maximum N_2/CO_2 selectivity 31.2 at 4 bar, followed by C_2H_6/CO_2 selectivity 21.2 at a different pressure 6 bar.

The solution–diffusion mechanism is an established theory in describing transport through dense nonporous membranes. The theory works well where interactions between the diffusing molecules and the membrane media have negligible effects on permeation and selectivity. Under ideal conditions, the gas permeation rate J_i (flux) and selectivity $\alpha_{i,j}$can be reliably predicted based on the knowledge of gas solubility and diffusivity in the transporting medium:

$$J_i = \frac{S_i D_i}{L}\Delta P = \frac{P_i}{L}\Delta P$$

$$\alpha_{ij} = \frac{P_i}{P_j} = \frac{S_i D_i}{S_j D_j}$$

Using the gas solubility and diffusivity data presented in Tables 2 and 4, the permeability and theoretical solution–diffusion selectivity for the 5 gas pairs in Fig. 7 are calculated and listed in Table 5, alongside the selectivity value calculated from the experimental permeation data. The value of gas solubility S_i is the reciprocal value of Henry's law constant adjusted for pressure unit from atm to mmHg.

Data in Table 5 presented a remarkable difference between the theoretically predicted perm-selectivity and the calculated perm-selectivity based on experimental gas flux data. There appears a diverse pattern of deviation from simple H_2, N_2 to CO_2 and C_2H_6, suggesting permeation and gas separation by SILM is strongly specific to the gas-ionic liquids combinations. The permeability of simple H_2 and N_2 is much faster than predicted values despite the two gases have very low solubility in the ionic liquid, suggesting transport of smaller, non-interactive gases are more likely diffusion controlled and less dependent on solubility. CO_2 has smaller observed permeation rate than the predicted values. The slow CO_2 diffusion is more likely influenced by strong CO_2-ILs interaction which impeded the motion of CO_2 molecules in the ionic liquid. The predicted and experimental permeation rate for CH_4 are very close considering the uncertainty associated with the absolute accuracy of the solubility data. CH_4 is non polar and considered non-interactive with the ionic liquid. Its permeation rate is influenced by combined gas dissolution and diffusion. It is the only gas molecule in this work which has experimental permeability value similar to the predicted value by the solution diffusion model. In contrast to CO_2, permeation of C_2H_6 is faster despite it has the smallest diffusion coefficient and a strong interactions with the ionic liquids, reflected by large dissolution enthalpy and entropy which is to be elaborated in the following section. However, the strong C_2H_6-IL interactions facilitated C_2H_6 transport rather than impeded the motion of the gas molecule, especially at increased gas phase pressure.

Table 4
Calculated gas diffusion coefficients based on Wilke–Chang and Scheibel model correlations in three ionic liquids ($D \times 10^{-6}\,cm^2 s^{-1}$).

Gas	CO_2	C_2H_6	CH_4	N_2	H_2
Ionic liquid	[C_4mim][NTf_2]				
Wilke–Chang [46]	3.55	2.97	3.48	3.61	4.13
Scheibel [47]	3.96	2.63	3.78	4.13	5.68
Gas molar volume (cm^3/mol) [51]	94.07	145.50	98.60	90.10	65.00
Gas molecular diameter (nm) [51]	0.399	0.439	0.378	0.367	0.291
Ionic liquid	[C_{10}mim][NTf_2]				
Wilke–Chang	2.01	1.68	1.97	2.05	2.34
Scheibel	2.66	1.74	2.54	2.78	3.85
Ionic liquid	[C_4mim][OTF]				
Wilke–Chang	1.95	1.63	1.92	1.99	2.27
Scheibel	2.02	1.36	1.93	2.10	2.87

Table 5
Corroboration and comparison of gas permeation rate and selectivity based on experimental permeation data and predictive calculations by solution–diffusion theory using independently measured gas solubility and diffusivity in [C_4mim][NTf_2] at T = 303 K.

Gas	CO_2	C_2H_6	CH_4	N_2	H_2
Molecular diameter (nm)	0.399	0.439	0.378	0.367	0.291
Measured gas solubility $S_i \times 10^5$ (mol mol^{-1} cm Hg^{-1})	36.84	3.82	1.45	0.93	0.24
Scheibel gas diffusivity $D_{i,j} \times 10$ (cm^2/s)	3.96	2.63	3.78	4.13	5.68
Predicted solution–diffusion permeability (barrer) $P_i = S_i \times D_i$	14.58	1.04	0.55	0.38	0.14
Experimental permeability (barrer) $P_i = \frac{J_i \Delta P}{L}$	2.3	3.4	0.43	72.6	20.1
Gas pairs	C_2H_6/CH_4	C_2H_6/CO_2	CH_4/CO_2	N_2/CO_2	H_2/CO_2
Predictive solution–diffusion selectivity $\alpha_{i,j} = \frac{P_i}{P_j} = \frac{S_i D_i}{S_j D_j}$	1.89	0.022	0.098	0.026	0.0096
Experimental based selectivity $\alpha_{i,j} = \frac{J_i}{J_j}$	7.35	1.45	0.19	31.57	8.16

For separation analysis, in the case of N_2/CO_2 pairs, a rather contrasting reversal of the predicted selectivity ($\ll$1.0) is found to the observed experimental selectivity ($\gg$1.0). Similar reversal of selectivity is also found for other gases pairing with CO_2. The molecular specific interactions between the diffusing gas molecules and the ionic liquid underpins the level of deviations from the solution–diffusion mechanism. On a comparative and qualitative understanding, the nature and strength of gas-ionic liquid interactions for simple (H_2, N_2, and CH_4), polar (H_2O, and CO_2) and more organic C_2H_6 can be revealed by examining the thermodynamic properties of gas dissolution enthalpy and entropy.

The Gibbs energy of solvation (ΔG^{∞}_{solv})is given by:

$$\Delta G^{\infty}_{solv} = \Delta H^{\infty}_{solv} - T\Delta S^{\infty}_{solv}$$

The variation with temperature of the solubility, expressed in Henry's law constant, is directly related to the thermodynamic properties of solvation. In the case of gaseous solutes at low pressure, it is practically identical to the thermodynamic properties of solution.

$$\Delta G^{\infty}_{solv} = RT \ln\left(\frac{K_H}{p^o}\right)$$

Therefore, the partial enthalpy (ΔH^{∞}_{solv}) and entropy (ΔS^{∞}_{solv}) between the two states can be calculated from the partial derivative of the Henry's law constants with respect to temperature at constant pressure:

$$\Delta_{sol} H^{\infty} = -RT^2 \frac{\partial}{\partial T}\left[\ln\left(\frac{K_H}{p^0}\right)\right]$$

$$\Delta_{sol} S^{\infty} = -RT \frac{\partial}{\partial T}\left[\ln\left(\frac{K_H}{p^0}\right)\right] - R \ln\left(\frac{K_H}{p^0}\right)$$

The calculated values of gas dissolution enthalpy and entropy are presented in Table 6.

Dissolution enthalpy and entropy for H_2 and N_2 in [C_4mim][NTf2] have not been found in literature. H_2 and N_2 has reported [55] solvation enthalpy −3.24 and −4.80 Jmol^{-1} K-1 (T = 293 K) respectively in ionic liquid [C4mim][BF4]. Carbon dioxide has stronger interactions at molecular level with [C_4mim][NTf_2], elicited from the greater dissolution enthalpy value of −13.86 kJ mol^{-1} (strong exothermic dissolution process), and large entropy of −75.29 Jmol^{-1} K^{-1}. C_2H_6 also has an exothermic dissolution enthalpy and large entropy at −62.22 Jmol^{-1} K^{-1}. The exothermic dissolution enthalpy value suggests that it has good affinity with the ionic liquids, derived from attractive van der Waal force between ethane and the alkyl chain on the cation. On the other hand, the entropic ethane can be disruptive to the order of cation–anion distribution. Low diffusivity and affinitive C_2H_6-IL interactions underlie a comparatively smaller C_2H_6 permeability at low gas phase pressure. The trend reversed, however, when C_2H_6 concentration increased inside the ionic liquid phase which led fastest

Table 6
Gibbs energy of solvation (ΔG^{∞}_{solv}), partial enthalpy (ΔH^{∞}_{solv}) and entropy (ΔS^{∞}_{solv}).

T/K	dG/kJ mol^{-1}	dH/kJ mol^{-1}	dS/J mol^{-1} K^{-1}	T/K	dG/kJ mol^{-1}	dH/kJ mol^{-1}	dS/J mol^{-1} K^{-1}
[C_4mim][BF_4] + CO_2				[C_4mim][NTf_2] + CO_2			
303	10.45	−14.42	−82.10	303	8.971	−13.79	−75.13
313	11.28	−14.62	−82.75	313	9.721	−13.67	−74.74
323	12.11	−14.81	−83.33	323	10.47	−13.56	−74.39
333	12.95	−14.98	−83.87	333	11.21	−13.46	−74.08
[C_4mim][BF_4] + C_2H_6				[C_4mim][NTf_2] + C_2H_6			
303	14.72	−9.21	−78.97	303	11.72	−7.13	−62.22
313	15.53	−10.75	−83.97	313	12.40	−10.96	−74.64
323	16.40	−12.19	−88.51	323	13.21	−14.54	−85.92
333	17.30	−13.55	−92.65	333	14.12	−17.92	−96.20
[C_4mim][BF_4] + CO				[C_4mim][NTf_2] + CO			
303	19.23	−6.92	−86.3	303	16.22	−5.59	−71.98
313	20.20	−13.46	−107.5	313	16.96	−6.89	−76.22
323	21.37	−19.60	−126.8	323	17.75	−8.11	−80.06
333	22.73	−25.37	−144.4	333	18.56	−9.26	−83.56

exponential increase in fluxes with pressure. It is thought that C_2H_6 molecules are well dispersed in the ionic liquids phase by "pegging" on the alkyl chains on the imidazolium cations, leading to dispersed phase and being disruptive to cation–anion distributions. The dispersed distribution of C_2H_6 molecules would have led to the fast permeation increase when C_2H_6 concentration inside the ionic liquids phase increased under high pressure, especially after the ionic liquids became saturated with no free "pegging" sites available for retention of the C_2H_6 molecules.

3.4. Ionic liquids specific gas selectivity

The pressure dependence of N_2/CO_2 selectivity is more pronounced in ionic liquid [C_4mim][NTf2]. However, gas feed pressure had almost no effect on N_2/CO_2 selectivity in ionic liquids [C_4mim][OTF] (Fig. 8) which shares the same cation but differs in anion. Contrasting to declining N_2/CO_2 selectivity with pressure in [C_4mim][NTf2], the N_2/CO_2 selectivity showed a slight increase with pressure in [C_{10}mim][NTf2] which has a larger cation and greater liquid free volume due to extended alkyl chain length. The results presented in Fig. 8 clearly points to molecular specific gas-ILs interactions leading to contrasting perm-selectivity performance in different gas-ILs combinations. It also suggest a discriminating gas selectivity based on molecular structure of ionic liquids and the molecular properties of the diffusing gas, suggesting a targeted approach to specific ionic liquid design for specific gas separations.

3.5. Further discussion on the special case of CO_2

CO_2 possess the highest solubility and a comparable diffusion coefficient among the five gases studied for permeation performance. It also has large dissolution enthalpy and entropy. If the prognosis, put forward previously to explain enhanced C_2H_6 permeation at high pressure, is applicable to the case of CO_2 transport through the SILM, then a greater CO_2 permeability than all other gases at high pressure is expected. In contrast, the CO_2 flux increase with pressure is much less pronounced, and its permeability remain the lowest at the high pressure range (Fig. 6). This reversed correlation between higher solubility and lower permeability at comparable diffusivity values suggests that CO_2 has different and specific molecular interactions with the ionic liquids.

CO_2 dissolution in the ionic liquids increases with pressure as shown by data from Anthony et al. [29] presented in Fig. 9. Although the increased CO_2 concentration in IL phase led to a higher CO_2 permeation, the increase is not strong enough to reverse the N_2/CO_2 selectivity. It is hypothesised that ionic liquids possess a condensing and holding capacity towards CO_2 which has a relatively low critical

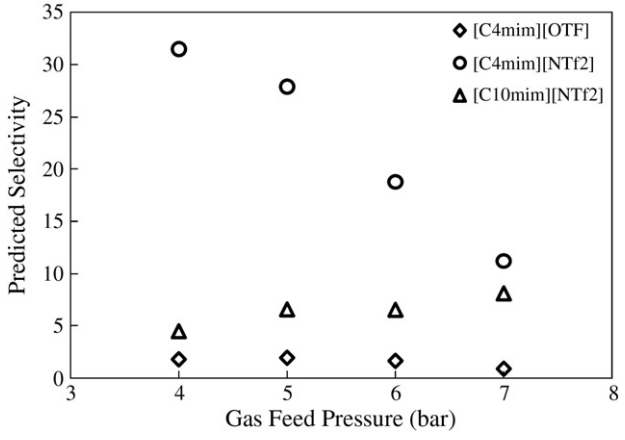

Fig. 8. Effects of three different ionic liquids on predicted N_2/CO_2 selectivity in SILMs.

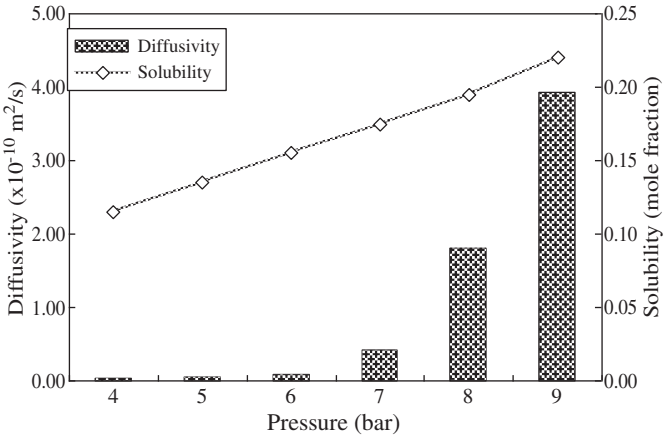

Fig. 9. Concentration dependence of solubility [courtesy of Anthony et al. Ref 29] and exponential increase of CO_2 diffusion coefficient in [C_4mim][NTf_2] SILM.

pressure of condensation in comparison to other simple gases, regardless the interactions with ILs. The high CO_2 solubility inside ionic liquids could be consequential effects of both chemo-sorption and partial condensation. This hypothesis leads to an interesting question of the state of existence of the accumulating CO_2 molecules in ionic liquids phase. By employing techniques for studying molecular dynamics, Hong et al. reported [56] that the partial radial distribution functions for the cation–anion distribution in [C_2mim][NTf_2] in the absence and presence of 20 mol% of acetonitrile have the same value which indicates that acetonitrile dissolved in IL within existing channels, and thus did not break the cation–anion structure. This was suggested to be due to the dipole movement of acetonitrile, and therefore could be the same for the carbon dioxide with quardpole movement. The analysis implies that high concentration of CO_2 in the SILM phase at elevated pressure does not necessarily leads to greater homogeneous dispersion of CO_2 in the ionic liquids phase, which is responsible for faster permeability according to the conventional solution diffusion theory. Rather, the residence of highly concentrated CO_2 molecules in the supported ionic liquids occupies the interstitial and hole free volume in the SILM structure, typified by voids or holes existed in glassy polymer structures. Moreover, it is speculated that pockets of concentrated CO_2 in the ionic liquid phase may be created by the condensing power of the ionic liquids which leads to formation of localized reservoirs of critical CO_2 fluids under a partial pressure much lower than the critical pressure required at the same temperature in gas phase.

When considering the diffusion coefficient in this SILM, it is necessary to point out the differences between dense polymer membrane and supported ionic liquid membrane. Since many reports revealed that ionic liquids possess properties of both a solid and a liquid [57], one may speculate a transformation of ILs from liquid to solid state might happen when the ILs are confined to nanoscale pores surrounded by functionalised polymers with high surface charge, which can exerts strong binding force on the cations and anions. Chen et al. [58] found that [C_4mim][PF_6] performs a fully different phase transition and crystal formation when confined in multiwalled nanotubes. It could be the similar situation in our NF membranes, that high electric charge density between the NF membrane materials and ionic liquids shorten the intermolecular spacing, thereby forming a more stable structure. The quardpole movement of CO_2 in this semi-solid membrane could be different as in bulk ionic liquids, and which could be another key factor leading to deviation from the solution diffusion theory based on solubility and diffusivity data obtained in bulk ionic liquid phase. The phase state of the ionic liquids after immobilisation inside the nano-scale pores surrounded by charged polymer groups is unclear, but it is an important issue for future SILM research.

3.6. Concentration dependence of diffusivity in SILMs

When gas transport through the SILM is governed by diffusion, Fick's second law dictates:

$$\frac{P_i}{RT}\frac{dV}{Adt} = -\frac{\phi}{\tau}D_i\frac{dc_i}{dx}$$

where ϕ is the porosity of a membrane, and τ is the membrane tortuosity factor. By applying gas law and performing integration, the diffusion coefficient can be calculated from:

$$V_t = D_i S_i \frac{ART}{L}\frac{\phi}{\tau}\frac{P_{i,F}-P_{i,P}}{P_i}(t-t_0)$$

Given a constant pressure and assuming membrane porosity 0.05 and tortuosity 1.55, by using the independently measured CO_2 solubility in [C_4mim][NTf_2] at different pressure by Anthony et al. [29], the change in CO_2 diffusion coefficient with changing feed gas pressure can be calculated from the gradient in plotting the linear relation between accumulated permeating gas volume V_t with time. t_0 is the experimentally observed lag time for the SILM to become saturated by the permeating gas before the onset of steady gas flux. The results shown in Fig. 9 demonstrate that the diffusion coefficient increases in an exponential fashion with increasing CO_2 concentration in the SILM phase, in contrast to the linear increase of CO_2 diffusion coefficient in pure ionic liquids [C_4mim][BF_4] and [C_4mim][PF_6] as reported in literature [44,45], which used the time lag method for the calculation of both gas solubility and diffusivity without independently measured values of both.

4. Conclusion

A framework analysis is put forward to address the interrelations between gas solubility, diffusivity and thermodynamic properties in ionic liquids to observed gas permeation and separation performance in SILMs, which are often complicated by the complex gas-ILs molecular interactions, leading to non-ideal behaviour and deviations from conventional solution–diffusion theory. SILMs by ionic liquids supported on nano-pore membranes possess high pressure stability unmatched by other SIMs or SILMs supported on micron-pore membranes. It offers opportunity to operate SILM at industrial relevant high pressure for gas separations, and allowed analysis of perm-selectivity performance which showed very different behaviour at high pressure to those reported for SILMs operating under atmospheric pressure. Increased gas concentration in the ionic liquids phase led to changes in transport properties, which are gas concentration dependent in the ionic liquid phase.

The permeability of CO_2, N_2, H_2, CH_4 and C_2H_6 increases in an exponential fashion with increasing gas feed pressure, with C_2H_6 showing the largest increase despite it has the lowest diffusivity in the ionic liquids. The affinitive molecular interaction between C_2H_6 and ionic liquids, demonstrated by exothermic dissolution enthalpy and cation–anion order disruptive entropy, contributed to the fastest increase in permeation rate with increased pressure. A hypothesis was put forward that C_2H_6 molecules could peg on the side alkyl chains on the imidazulium [$C_n$mim] cation because of high chemical affinity between the hydrocarbons. Unlike CO_2 which aggregates inside ionic liquid phase, C_2H_6 molecules could be well dispersed throughout the ionic liquid phase. When ionic liquids were saturated with the C_2H_6 molecules at high pressure, they lost "binding" capacity to hold on to gas molecules, and the permeation rate showed explosive increase, a typical pattern for concentration-dependent transport.

Independently measured gas solubility and diffusivity in ionic liquids were applied to analysing gas permeation and separation through supported ionic liquids by the conventional solution–diffusion theory, and attempt was made to corroborate the theoretically predicted permeability and selectivity to experimentally observed gas permeation rate and separation factor. The analysis revealed a large and varied deviation between the theory and experimental outcome, and the deviation is specific to gas-IL combinations which determine the nature of gas-IL interactions. Permeation for simple non-polar gases H_2 and N_2 appears to be diffusion controlled. CO_2 has the lowest permeability and a reversed N_2/CO_2 selectivity in spite of CO_2 possessing the highest solubility, comparable diffusivity and a large exothermic dissolution enthalpy and entropy. This leads to an understanding that the nature of CO_2-ILs interactions is very different to that of ethane and other simple gases. The large CO_2 dissolution in the SILM and its increased solubility coefficient with pressure may be a consequence of a special condensing and "holding capacity" for CO_2 by the ionic liquids. The residing state of CO_2 in [C_4mim][NTf2] is not homogeneously dispersive. Unlike C_2H_6, dissolved CO_2 may not peg on the alkyl chains, and not as disruptive to cation–anion distributions. Rather it exists in pockets of aggregated CO_2 molecules in between the well coordinated and structured cation–anion groups. Compared to the linear increase of CO_2 solubility with pressure, effective diffusivity was found to increase in an exponential fashion, suggesting CO_2 diffusion coefficient in the membrane phase is not constant but also concentration dependent.

The experimental results for gas permeation through the SILMs using three different ionic liquids, typified by different N_2/CO_2 selectivity performance in ionic liquids [C_4mim][NTf2], [C_4mim][OTF] and [C_{10}mim][NTf2], also demonstrate that ionic liquids possess discriminating properties towards gas dissolution and transport due to molecular specific interactions. The transport and separation by molecular specific nature could be explored for targeted approach to ionic liquid design for future gas separations.

Nomenclature

$\alpha_{i,j}$	gas selectivity/separation factor	
a_1	radius of the solute	(cm)
c_i	gas mole fraction in SILMs	
D_i	diffusivity	($cm^2\ s^{-1}$)
ΔG^{∞}_{solv}	The Gibbs energy of solvation	($Jmol^{-1}K^{-1)}$
ΔH^{∞}_{solv}	partial enthalpy of solvation	($Jmol^{-1}K^{-1}$)
J_i	Gas permetaion rate/flux	($cm^3s^{-1}cm^{-2}$)
k	Boltzmann's constant	($J\ K^{-1}$)
K_H	Henry's law constant	(atm/mmHg)
L	membrane thickness	(cm)
M_i	molecular weight	($g\ mol^{-1}$)
P_i	permeability	(barrer)
p	pressure	(bar)
S_i	solubility	($mol\ mol^{-1}\ cmHg^{-1}$)
ΔS^{∞}_{solv}	partial entropy of solvation	($Jmol^{-1}K^{-1}$)
T	temperature	(K)
$\overline{V}_1$	molar volume of gas solute	($cm^3\ mol^{-1}$)
V_{bulb}	volume of gas bulb	($cm^3\ mol^{-1}$)
μ_2	solution viscosity	(mPa s)
ϕ_2	fugacity coefficient	
δ	deviation	

Acknowledgement

The authors would like to acknowledge QUILL for providing a scholarship to Y Zou for this project.

References

[1] Welton T. Coord Chem Rev 2004;248:2459.
[2] Zhang ZC. Advances in Catalysis, Volume 49; 2006. p. 153–237.
[3] Pandey S. Anal Chim Acta 2006;556:38.
[4] Hanioka S, Maruyama T, Sotani T, Teramoto M, Matsuyama H, Nakashima K, et al. J Membr Sci 2008;314:1.
[5] Ortiz A, Ruiz A, Gorri D, Ortiz I. Searation Purif Technol 2008;28:311.

[6] Kang SW, Lee DH, Park JH, Char K, Kim JH, Won J, et al. J Membr Sci 2008;322:281.
[7] Figoli A. Liquid Membr 2010:327.
[8] Krull FF, Fritzmann C, Melin T. J Membr Sci 2008;325:509.
[9] Fortunato R, Afonso CAM, Benavente J, Rodriguez-Castellón E, Crespo JE. J Membr Sci 2005;256:216.
[10] Scovazzo P, Kieft J, Finan DA, Koval C, DuBois D, Noble R. J Membr Sci 2004;238:57.
[11] Gan Q, Rooney D, Xue M, Thompson J, Zou Y. J Membr Sci 2006;280:948.
[12] Park YI, Kim BS, Byun YH, Lee SH, Lee EW, Lee JM. Desalination 2009;236:342.
[13] Bara JE, Gabriel CJ, Carlisle TK, Camper DE, Finotello A, Gin DL, et al. Chem Eng J 2008;321:3.
[14] Scovazzo P. J Membr Sci 2009;343:199.
[15] Jiang A, Zhou Z, Jiao Z, Li L, Wu Y, Zhang Z. J Phy Chem B 2007;111:5058.
[16] Pennline HW, Luebke DR, Jones KL, Myers CR, Morsi BI, Hentz YJ, et al. Fuel Proc Technol 2008;89:897.
[17] Myers C, Pennline H, Luebke D, Ilconich J, Dixon JK, Maginn EJ, et al. J Membr Sci 2008;322:28.
[18] Dai S, Depaoli D, Dietz M, Mays J, MacFarlane J, Steele W. Chemical industry vision 2020 technology partnership workshop; 2003.
[19] Yokozeki A, Shiflett MB. Appl Energy 2007;84:351.
[20] Scovazzo P, Havard D, McShea M, Mixon S, Morgan D. J Membr Sci 2009;327:4.
[21] Gan Q, Xue M, Rooney D. Sep Purif Technol 2006;51:185.
[22] Ballerat-Busseroles K, Costa Gomes MF, Husson P, Jacquemin J, Majer V. Padua AAH, CHISA 2004 — 16th International Congress of Chemical and Process Engineering, Prague, Rép. Tchèque; 2004. p. 9009.
[23] Blanchard LA, Hancu D, Beckman EJ, Brennecke JF. Nature 1999;399:28.
[24] Dyson PJ, Laurenczy G, Ohlin CA, Callance J, Welton T. Chem Commun 2003:2418.
[25] Ohlin CA, Dyson PJ, Laurenczy G. Chem Commun 2004:1070.
[26] Heintz A, Verevkin SP. J Chem Eng Data 2005;50:1515.
[27] Aki SNVK, Mellein BR, Saurer EM, Brennecke JF. J Phys Chem B 2004;108:20355.
[28] Perdew JP. Phys Rev B 1986;33:8822.
[29] Anthony JL, Anderson JL, Maginn EJ, Brennecke JF. J Phys Chem B 2005;109:6366.
[30] Jiang Y, Zhou Z, Jiao Z, Li L, Wu Y, Zhang Z. J Phys Chem B Lett 2007;111:5058.
[31] Cadena C, Anthony JL, Shah JK, Morrow TI, Brennecke JF, Maginn EJ. J Am Chem Soc 2004;126:5300.
[32] Chen Y, Zhang S, Yuan X, Zhang Y, Zhang X, Dai W, et al. Thermochim Acta 2006;441:42.
[33] Shiflett MB, Yokozeki A. Ind Eng Chem Res 2005;44:4453.
[34] Huang J, Riisager A, Berg RW, Fehrmann R. J Mol Catal A Chem 2008;279:170.
[35] Dyson PJ, Laurenczy G, André Ohlin C, Vallance J, Welton T. Chem Commun 2003: 2418.
[36] Ahlrichs R, Bar M, Haser M, Horn H, Kolmel C. Chem Phys Lett 1989;162:165.
[37] Vosko SH, Wilk L, Nusair M. Can J Phys 1980;58:1200.
[38] Schafer A, Huber C, Ahlrichs R. J Chem Phys 1994;100:5829.
[39] Klamt A, Jonas V, Burger T, Lohrenz JC. J Phys Chem A 1998;102:5074.
[40] COSMOthermX Manual, COSMOlogic GmbH & Co KG, Leverkusen, Germany
[41] Finotello A, Bara JE, Camper D, Noble RD. Ind Eng Chem Res 2008;47:3453.
[42] Jacquemin J, Husson P, Majer V, Costa-Gomes MF. J Sol Chem 2007;36:967.
[43] Muldoon MJ, Aki SNVK, Anderson JL, Dixon JK, Brennecke JF. J Phys Chem B 2007;111: 9001.
[44] Taveira P, Mendes A, Costa C. J Membr Sci 2003;221:123.
[45] Morgan D, Ferguson L, Scovazzo P. Ind Eng Chem Res 2005;44:4815.
[46] Wilke CR, Chang P. AIChE J 1955;1:264.
[47] Scheibel EG. Ind Eng Chem 1954;46:2007.
[48] Buzzeo MC, Klymenko OV, Wadhawan JD, Hardacre C, Seddon KR, Compton RG. J Phys Chem A 2003;107:8872.
[49] Yokozeki A, Shiflett MB. Appl Energy 2007;84:351.
[50] Perry RH, Green DW. Perry's chemical engineering handbook. 7th edition. New York: McGraw-Hill; 1997.
[51] Seader JD, et al. Separation process principles. John Wiley & Sons, Inc; 1998.
[52] Wang R. J Membrane Sci 2002;198:259.
[53] Pandey P. Prog Polym Sci 2001;26:853.
[54] Pino M. Polymer 2005;46:4886.
[55] Jacquemin J, Costa Gomes MF, Husson P, Majer V. Chem Thermodyn 2006;38:490.
[56] Hong G, Jacquemin J, Husson P, Costa-Gomes MF, Deetlefs M, Nieuwenhuyzen M, et al. Ind Eng Chem Res 2006;45:8180.
[57] Kroon MC, Shariati A, Costantini M, van Spronsen J, Witkamp GJ, Sheldon RA, et al. J Chem Eng Data 2005;50:173.
[58] Chen S, Wu G, Sha M, Huang S. J Am Chem Soc 2007;129:2416.